



Sorption of Cu(II), Zn(II) and Ni(II) from aqueous solution using activated carbon prepared from olive stone waste

Gehan E. Sharaf El-Deen

Radioactive Waste Management Department, Hot Laboratories Center, Atomic Energy Authority, Egypt.

ARTICLE INFO

Article history:

Received 15 June 2016
revised form 4 July 2016
Accepted 6 August 2016

Keywords:

Sorption
Cu(II)
Zn(II)
Ni(II)
Physically activation Olive stone

ABSTRACT

The performance of olive stone activated carbon (OSAC) for the sorption of Cu^{2+} , Zn^{2+} and Ni^{2+} ions was investigated via batch technique. OSAC materials were prepared under different physical activation conditions. Olive stone waste was activated with N_2 and steam at 900°C at a 3.5h hold time (OSAC-3). The characterization for OSAC-3 was performed under BET-surface area, SEM, density and FTIR-spectrum. The optimum adsorption conditions were specified as a function of agitation time, initial metal concentration, pH, and temperature. The kinetic results were found to be fast and described well by the pseudo-second order model. The adsorption capacities were 25.38mg/g (Cu^{2+}), 16.95mg/g (Zn^{2+}) and 14.65mg/g (Ni^{2+}) which followed the sequence $\text{Cu}^{2+} > \text{Zn}^{2+} > \text{Ni}^{2+}$. The spontaneous adsorption for all the studied cations, endothermic nature for both Zn^{2+} and Ni^{2+} ions and exothermic nature for Cu^{2+} ions were obtained. The results showed that OSAC-3 is an economically feasible material for Cu^{2+} , Zn^{2+} and Ni^{2+} remediation from weak acidic contaminated effluents.

1. Introduction

Environmental pollution by heavy metals like As, Cd, Co, Cr, Cu, Hg, Ni, Pb, Sn, Zn, etc. is a matter of ever-growing concern because of their toxicity. Even relatively low concentrations can have long term health effects on humans [1]. Heavy metals appear in wastewater discharged from different industries, including smelting, metal plating, Cd-Ni batteries, electronic industry, electroplating, metal finishing plants, phytopharmaceutical plants, phosphate fertilizer, mining pigments, stabilizer alloy manufacturing, and many others [2]. Trace amounts of copper, zinc, and nickel are essential for humans, microorganisms, and animals. However, an excessive intake of copper will cause stomach upset, ulcers, mental retardation as well as liver and brain damage in humans [1]. The consumption of nickel that exceeds permissible levels can cause various diseases like lung and nasal cancers, pulmonary fibrosis, renal edema, lung cancer, skin dermatitis, diarrhea, nausea and vomiting [3]. Elevated concentrations of zinc can cause

several health problems, e.g., arteriosclerosis, pancreas damage, vertigo, and disharmony [4]. The US Environmental Protection Agency (EPA) requires the level of copper, zinc, and nickel in drinking water not to exceed 1.3, 5, and 0.04 mg/L, respectively [5]. Also, excessive amounts of these elements are harmful for the environment. Various treatment technologies such as flotation, electrochemical methods, coagulation, filtration, precipitation, adsorption, ion exchanges, reverse osmosis and membrane technologies have been employed to remove hazardous heavy metals from aqueous solutions [6]. However, most of these processes have some drawbacks such as high operating costs, the inability to remove toxic elements from a wide range of wastewaters, and their ineffectiveness in lower concentrations [7]. Adsorption on activated carbons is considered as one of the most practical, easy to operate, environmentally friendly, and economical approach for water treatment. The utilization of low-cost agro-industrial waste as a precursor for the production of activated carbon supports the economic feasibility of this adsorbent. It has

*Corresponding author. Tel: +2 012 00301939
E-mail address: gsharaf2000@gmail.com

been shown that specific surface area and porosity are not the only determinant parameters in activated carbon. Surface chemistry is also an effective parameter in the process of metal ions adsorption. Accordingly, activated carbon surfaces can be improved by acidic treatment, oxidation, heating or ammonization to enhance metal species removal [8]. Activated carbons (AC) are used as adsorbent materials because of their large surface areas, high degree of surface activates, microporous structures and high adsorption capacities [9]. As of today, the use of commercially produced activated carbons is still limited due to the high cost of raw materials such as coal and non-renewable materials. Efforts are being made with numerous researchers to produce more effective, cheaper, and environmental friendly activated carbons [10-14]. Therefore, various precursors such as agricultural and agro-industrial by-products materials have been used as precursor materials for activated carbon production by using various physical and chemical activation processes for preparations. One objective of this study is to prepare a more effective, economical, and environmental friendly activated carbon. Olive stone waste as a raw material for the production of activated carbon could be considered as a better choice among agro-industrial wastes because it is abundant and inexpensive, especially in Mediterranean countries. Olive stone waste, a by-product generated from olive oil extraction, are available in large amounts in Mediterranean countries like Egypt, where about 13,500 x130 tones per year are produced. This olive waste which is generated in huge quantities in a short period of time from November to March creates an environmental problem for Egypt [15]. The main use of this biomass is the production of energy. In addition to utilizing olive stone by-product as activated carbon, other uses that are been investigated include furfural production, biosorbent, abrasive, cosmetic, plastic filler, animal feed, or resin formation [16]. Another objective of the present work is to investigate the potential effectiveness of olive stone activated carbon (OSAC) on the removal of Cu^{2+} , Zn^{2+} , and Ni^{2+} ions from contaminated water at different conditions of physical activation in batch technique. At optimum conditions for OSAC-preparation, the effects of agitation time, initial concentration, initial solution pH, and thermodynamic parameters on the sorption capacity of OSAC were studied.

2. Materials and methods

2.1. Chemicals, Materials and Equipments

To perform the sorption experiments, 1000mg/L of copper, zinc and nickel standard solutions were prepared from $\text{CuCl}_2 \cdot 2\text{H}_2\text{O}$, $\text{ZnSO}_4 \cdot 7\text{H}_2\text{O}$ and $\text{Ni}(\text{NO}_3)_2 \cdot 6\text{H}_2\text{O}$ (Merck) using bi-distilled water. All chemicals used were of analytical grade purity. The olive stone waste was obtained from the by-product of olive oil producing factories in Wahet Sewa, Egypt. Ultra-pure nitrogen gas was employed for the activated carbon production. A high

temperature tube furnace (model CD-1700G, Chida, China) was used for preparing the OSAC-samples, while an Atomic absorption spectrophotometer (Hitachi model Z-8100, Germany), a Fourier Transform Infrared Spectrophotometer (NICOLET 380-FTIR, Thermo-scientific, UK), and a Scanning Electron Microscope were used for measuring. Nitrogen adsorption/desorption isotherms at 77 K on an automatic adsorption instrument (Nova 3200 BET instrument, Quanta chrome, Corporation, USA) were used for measuring surface area, average pore diameter, and total pore volume.

2.2. Preparation of sorbent:

The olive stone waste was supplied by an olive oil factory in the Wahet Sewa region of Egypt. This agro-industrial olive stone waste was dried in the sun, crushed and sieved. The granules of olive stone waste with diameter fractions from 0.7 to 2mm were used as a precursor for the production of activated carbon by a physical activation process at different conditions. Carbonization and activation are the two main steps in the physical activation process. These steps were followed to prepare different samples of OSAC and are summarized in Table (1). The preparation conditions for one of these samples can be explained as follows: carbonized olive stone waste was obtained by heating 100 gram of the clean dry crushed olive stone waste (as the original weight) to a specified temperature of 850°C at a rate of 50°C/10min. for a one hour hold time under flowing N_2 gas at 10psi. in a tube furnace (with inclined position of angle 70°); then, it was cooled to room temperature. In the activation step, the obtained samples from the last step were placed in the reactor, which was situated in the hot zone of the tubular furnace. Next, pure steam was introduced through the sample. The temperature was raised gradually (100°C/10min.) up to 450°C to allow free evolution of volatiles. The heating continued until 900°C for a 3.5h. hold time, then it was cooled and the weight determined. The granular activated carbon final product was crushed until its particle diameter was lower than 0.7mm, this was determined by sieving. After that, the granular activated carbon was kept in a closed bottle for further tests.

3. Characterization of olive stone activated carbon

The physical characterizations (specific surface area, carbon yield percent, weight loss, activation burn off, density), chemical characterizations (surface pH and the percent of oxides in ash-residue obtained by EDX), FTIR, and SEM were analyzed.

3.1. Physical characterizations of OSAC-3 product

Most of the physical properties for all the prepared OSAC were measured and are shown in Table 1. The one which had a higher surface area (OSAC-3) was selected for further investigations, and its physical properties were studied in

detail. The calculated specific surface area ($S_{\text{BET}}=850 \text{ m}^2/\text{g}$), total pore volume ($V_t=0.47 \text{ cc/g}$) and average pore radius ($r^*=11 \text{ \AA}$) were determined by the nitrogen adsorption-desorption isotherms.

The activation burn-off, yield percent and the weight loss due to activation were found to be 48.37%, 12.22% and 76.33g, respectively. The OSAC-3 reported good bulk density ($B_d=0.67 \text{ g/ml}$) and an apparent density (A_d) of 0.42g/ml. An adequate bulk density can help to improve the rate of filtration.

3.2. Chemical characterizations of OSAC-3 product

For pH determination of the OSAC-3 active surface, 1.0g of the dry carbon sample was stirred with 100ml of bi-distilled

water for 5h., then soaked for 3 days for equilibrate in a stoppered glass bottle. At end of this period, the pH of the carbon slurry was recorded after 3min. in order for the pH probe to reach equilibrium. It was observed that a neutral OSAC-3 surface with a pH of 7.2 was obtained. Therefore, its pH does not affect the aqueous medium during the sorption process. An EDX-analysis was important for determining the main oxides included in the ash content, shown in Table 2, in which K^+ and Ca^{2+} are the major alkaline ingredients of the ash residue of OSAC-3.

Table 1. Preparation conditions for synthesis of different OSAC-materials.

Sample no.	1. Carbonization step	$S_{\text{BET}}, \text{m}^2/\text{g}$	$V_t, \text{cc/g}$	$r^*, \text{\AA}$	$B_d, \text{g/cm}^3$
	2. Activation step				
OSAC-1	(1) 50°C/10min. at 850°C for 2h. (h.t).	530	0.283	21.3	0.837
	(2) 100°C/10min. with CO_2 gas at 825°C/2h. (h.t).				
OSAC-2	(1) 50°C/10min. at 850°C for 2h. (h.t).	780	0.533	15.50	0.677
	(2) 100°C/10min. with steam gas at 825°C/3h. (h.t).				
OSAC-3	(1) 50°C/10min. with N_2 -gas at 850°C for 1h. (h.t).	850	0.470	11.00	0.671
	(2) 100°C/10min. with steam gas at 900°C/3.5h. (h.t).				
OSAC-4	(1) 50°C/10min. with N_2 -gas at 850°C for 2h. (h.t).	300	0.180	11.70	0.731
	(2) 100°C/10min. with steam gas at 950°C/3.5h. (h.t).				
OSAC-5	(1) 50°C/10min. at 850°C for 1h. (h.t).	458	0.235	10.26	0.779
	(2) 100°C/10min. with steam gas at 900°C/3.5h. (h.t).				

(h.t= hold time)

Table 2. Main Oxides composition of OSAC-3 from EDX analysis

Units	Mg	Al	Si	P	S	Cl	K	Ca	Fe
%	1.9	1.1	3.6	3.4	8.3	7.1	56.1	16.7	1.8

3.3. Scanning electron microscope analysis (SEM)

The surface physical morphology of OSAC-3 activated carbon was examined using a scanning electron microscopy (S-2150, Hitachi High-Technologies) with 1600X magnification; it is shown in Fig. 1. The SEM micrograph clearly revealed that the dark cavities signified pores and the greyish areas were due to the carbon matrix. The reason for the formation of the cavities on the OSAC-3 sample may occur because during pyrolysis (carbonization process) the cellulosic structure loses small molecules as volatile materials such as water and carbon dioxide together with a complexity of aliphatic acids, carbonyls, alcohols, etc. These desired activations don't occur at a single decomposition temperature, but over a range of temperatures. Small molecules are removed from the original macromolecule of the network and the resultant porosity created [16].



Fig. 1. SEM of OSAC-3 activated carbon

As a result, a new lattice is continuously created with a composition of high C/H and C/O ratios. In regard to the carbonization of cellulosic materials, the obtained char and coal is microporous, but the micro pores may become filled or partially blocked with tars and other decomposed materials. The process used to create high porosity from low-porosity-carbonized material is known as "activation". This is usually completed by reaction with steam or carbon dioxide above 800°C, where the gas molecules penetrate the interior of the char particle to remove carbon atoms and the tar matter [17].

3.4. Fourier-Transform Infrared Spectroscopy (FTIR) The FTIR spectrum of the olive stone waste before activation is displayed in Fig.2(a). A broad absorption band at a wavenumber ranging from 3500 to 3200 cm^{-1} with a maximum absorption at about 3384 cm^{-1} means there is O—H stretching vibration owing to intermolecular hydrogen bonding. This band is observed in the spectra of carboxyl, phenols or alcohols groups and adsorbed water. An

absorption band at 2925 cm^{-1} is due to the aliphatic —CH group. The stretching —C=O group in normal ester was obtained at 1735 cm^{-1} , the conjugation interfered with possible resonance with the carbonyl group that led to an increase in the absorption frequency for the C=O band to appear at the 1738 cm^{-1} band. A weak band at 1670 to 1640 cm^{-1} was assigned to —C=O stretching vibrations of amides (—C=O—N). A strong band at 1035 cm^{-1} with a shoulder at 1259 cm^{-1} was associated to aliphatic ether (—C—O—); an ether group was obtained from alcohol (R—OH) or ester (—C=O) groups. The FTIR spectrum of OSAC-3 after activation, Fig.2 (b), showed that in comparison to the non-activated raw material, more peaks appeared at the OSAC-3 and some disappeared due to the cracking of some bonds by heating; the settling of broad bands at 3713–3683 cm^{-1} could be due to the NH_2 stretching vibration of the nitrile functional groups. A broad band at 3448 cm^{-1} was assigned to the stretching vibration of hydrogen bonded hydroxyl groups (—OH). A band appeared at 2367- 2369 cm^{-1} and was perhaps due to the —C≡C group. A band at 2337 cm^{-1} may be due to a weak nitrile group attached to the aliphatic chain [18]. Bands around 1705 cm^{-1} may be due to ketone or ketene. A band at 1466 cm^{-1} was assigned to stretching vibration of aliphatic —CH₂.

4. Results and discussion

4.1. Batch sorption procedure

Sorption experiments were carried out at 22±1°C by shaking a fixed amount (0.03g) of olive stone activated carbon in 50ml of metal solution in a thermostatic water bath mechanical shaker. The water bath was used to maintain a constant temperature. After equilibrium, the solid was filtered and the final heavy metal concentration as well as in the initial solution was measured by flame atomic absorption spectrometer (FAAS) (Hitachi Z-8100). The sorbed cations were determined from the difference between the initial and final concentration in the solution. The capacity of metal ions as sorbates was calculated as:

$$q_e = \frac{V(C_o - C_e)}{m} \quad (1)$$

where m (g) is the weight of olive stone activated carbon, V (L) is the solution volume, and C_o and C_e (mg/L) are the initial and equilibrium bulk ion concentrations, respectively. Initially, a preliminary test was performed to select the best OSAC-adsorbent for removing the investigated cations at a pH of 6. The results presented in Fig.3 indicate that OSAC-3 was the best adsorbent for the removal of the studied cations. Thus, OSAC-3 was selected to complete the remaining tests to study the optimum conditions for removing the investigated cations.

4.2. Effect of pH

The removal of heavy metals as pollutants from wastewaters by adsorption is highly dependent on the pH

of the solution, which affects the adsorbent surface charge, the degree of ionization and speciation of the adsorbate. The effect of solution pH on the sorption of heavy metals was investigated by using 0.03 g of OSAC-3 and 20 mg/L of metal ion concentration at initial pH values ranging from 2.5

to 9.2 for a 3 h shaking time at 295 K; the results are shown in Fig. 4. At a pH from 2.5 to 4, the sorption of metals onto the activated carbon was found to be low. This could be due to increasing the competition between the studied cations with H_3O^+ ions on active sites at a lower pH.

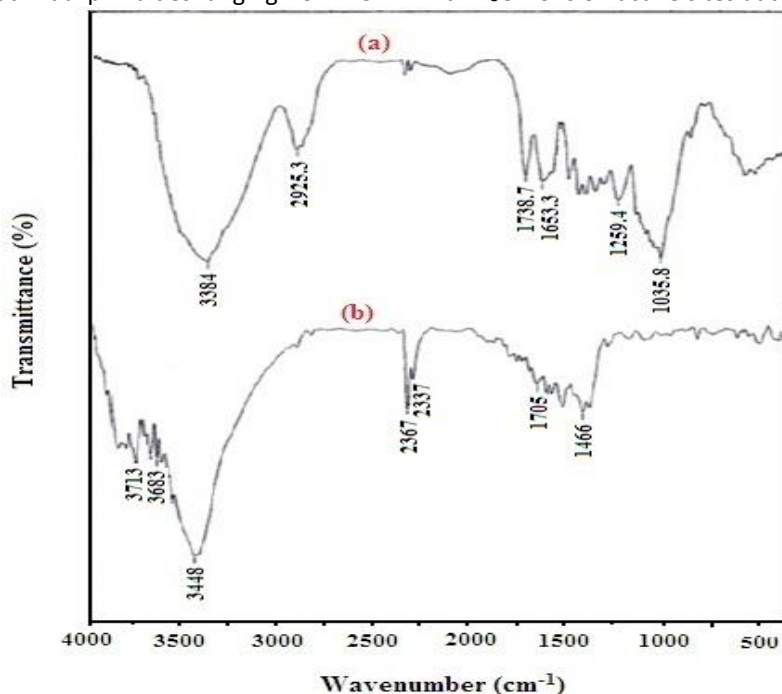


Fig. 2. FTIR spectra for original olive stone waste (a) and for OSAC-sample (b).

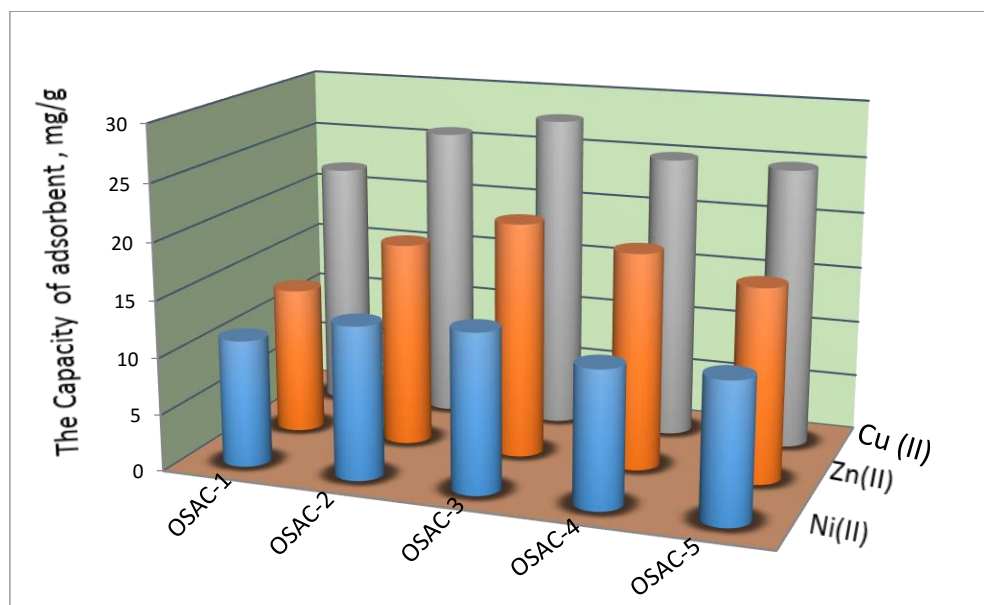


Fig. 3. Preliminary test results to select the best adsorbent to remove Cu(II), Zn(II) and Ni(II)-ions.

Metal uptake increased gradually with increasing pH from 4 to 7.2 for Cu^{2+} ions, and from 4 to 8 for Zn^{2+} and Ni^{2+} ions. This may be attributed to an increase in pH. More active sites with negative charges were expected to be exposed and this would attract the positively charged Cu(II), Zn(II) and Ni(II) ions for binding. The predominant species were Cu^{2+} , $Cu(OH)^+$, Zn^{2+} , and Ni^{2+} at a pH lower than 7.2, as shown in Fig. 6(a,b,c). Then, with increasing of the basicity

of the solution, the efficiency of the sorption process reached a steady state for Cu^{2+} ions after a pH of 7.2. But the sorption capacities for Zn^{2+} and Ni^{2+} ions drastically increased with increasing pH values from 7.5 to 9.2. This may be attributed to reducing the solubility and starting precipitation of the metal ions at higher pH-values [19] through the formation of $Cu(OH)_2$, $Zn(OH)_2$ and $Ni(OH)_2$ as precipitate at a pH higher than 7.5 and is shown in Fig.6

(a,b,c). Therefore, metal ions may accumulate inside the activated carbon porous or cracks by a mechanism known as combined sorption-micro precipitation [20]. Hence, the

next tests were carried out at an initial pH value of 5.7 to insure that no precipitation occurred for the studied cations.

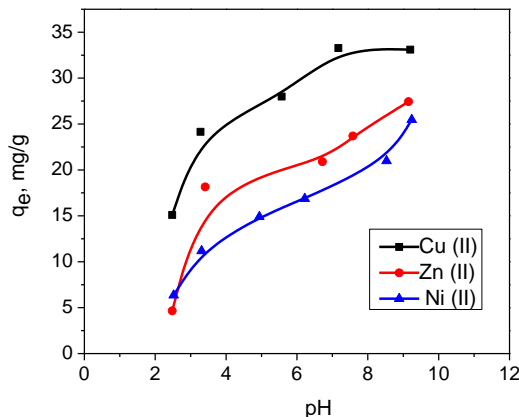


Fig. 4. Effect of pH on sorption of Cu²⁺, Zn²⁺ and Ni²⁺ ions on OSAC-3

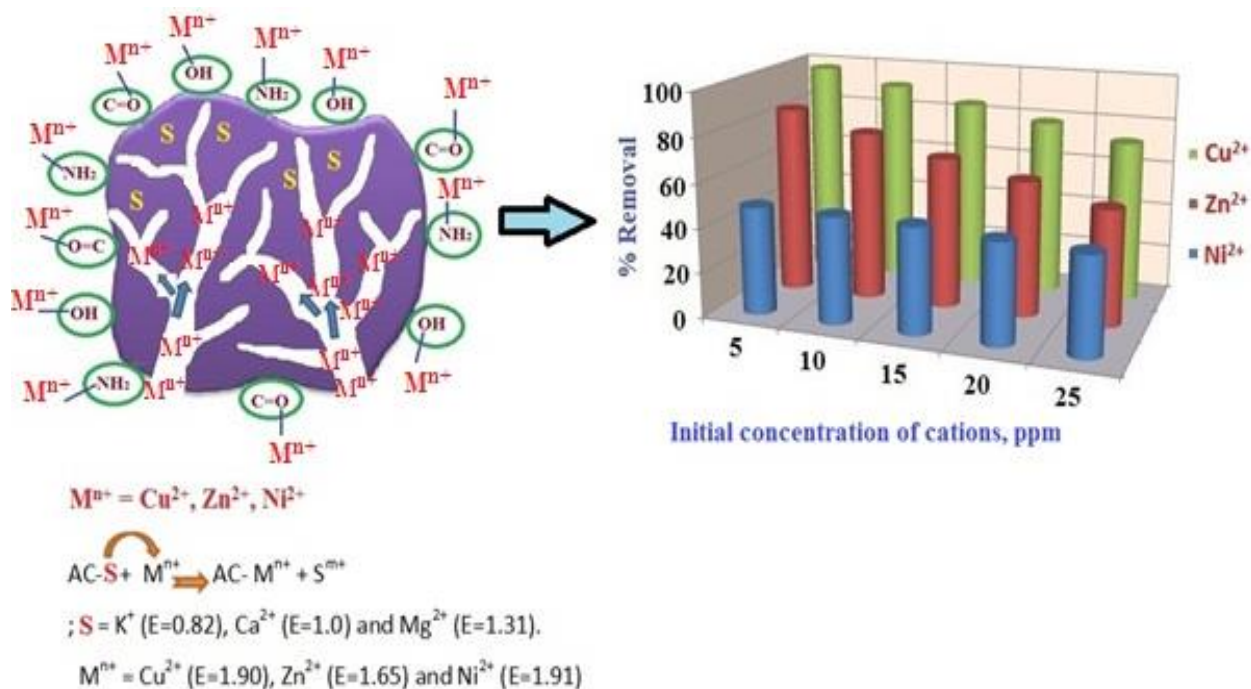


Fig. 5. Scheme of sorption mechanism and the % removal of Cu²⁺, Zn²⁺ and Ni²⁺ ions.

4.3. Effect of agitation time

To investigate the effect of agitation time on the sorption of the investigated cations from a weak acidic medium at a pH of 5.7, the experiments were conducted with a constant concentration of salt solution (20ppm). The plots, Fig. 7, show that the sorption equilibrium of the studied cations were reached after 30min. (for Cu²⁺ ions), less than 60min. (for Zn²⁺) and at 120min. (for Ni²⁺ ions) of agitation time. All the studied cations were fast removed in the first 5min., this may be attributed to the pores of OSAC-3 that were nearly completely blocked by the ions in the first 5min. Therefore,

two hours were designated for the subsequent studies to ensure complete equilibrium.

4.3.1. Sorption kinetic studies

In order to investigate the behavior of the sorbent and also to determine the rate controlling mechanism of the adsorption process, three sorption kinetic models are used: pseudo-first order, pseudo second order, and the intraparticle diffusion models. The Lagergren pseudo-first order model [21] is described by the following equation:

$$\log (q_e - q_t) = \log q_e - \frac{k_{ad}}{2.303} t \tag{2}$$

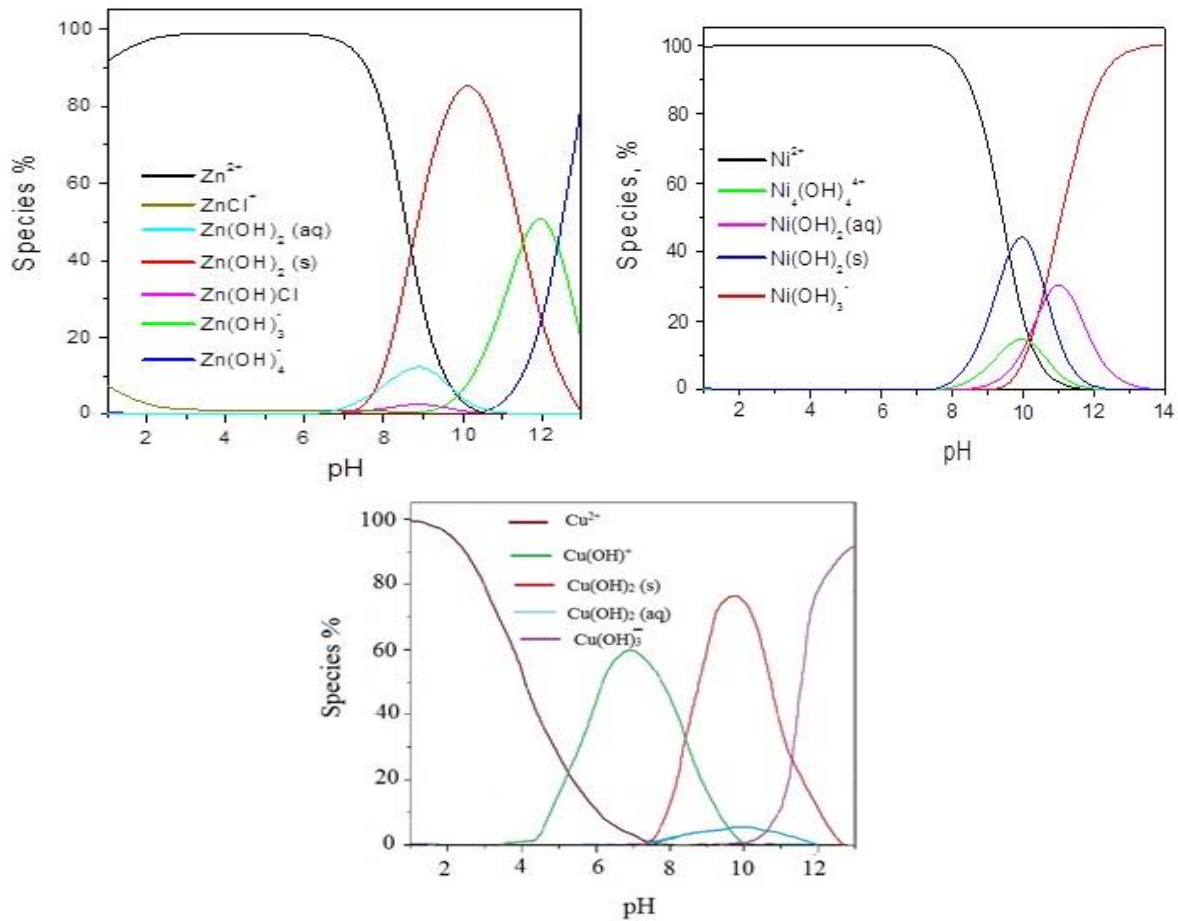


Fig. 6 (a,b,c). Speciation of Cu^{2+} , Zn^{2+} and Ni^{2+} in water obtained using the PHREEQC model according to metal concentration 20mg/L.

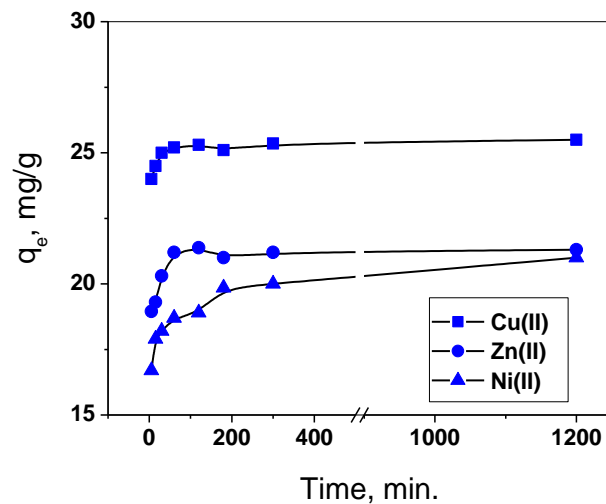


Fig. 7. Effect of agitation time sorption of Cu^{2+} , Zn^{2+} and Ni^{2+} on OSAC-3

where q_e (i.e. $q_{e,cal.}$) (mg/g) and q_t are the amounts of adsorbed cations on the surface of OSAC sorbent at equilibrium and at time t , respectively; k_{ad} is the Lagergren rate constant (min^{-1}). The plot of $\log(q_e - q_t)$ versus t (min.) in Figure (8) shows that straight lines are obtained for the studied cations. The first order rate constant, k_{ad} , and q_e are determined and listed in Table 3. In addition, the

experimental uptake ($q_{e,exp.}$) and the correlation coefficient (R^2) are also shown. It was noticed that the calculated uptake ($q_{e,cal.}$) values for all the investigated cations are not a match with the experimental data ($q_{e,exp.}$). The wide variation referring to the pseudo-first-order kinetic model did not fit the experimental data for the sorption of the studied cations by OSAC-3.

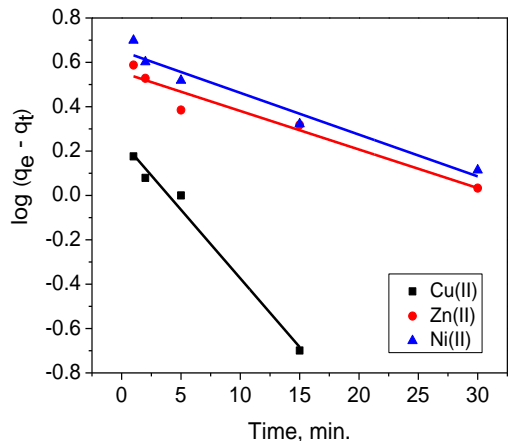


Fig. 8. Pseudo first order kinetic model for sorption of Cu²⁺, Zn²⁺ and Ni²⁺-ions on OSAC-3

The chemisorption pseudo-second order model proposed by Hall et al. (1966) [22] is described by equation Eq. (3):

$$\frac{t}{q_t} = \frac{1}{k_2 q_e^2} + \frac{1}{q_e} t = \frac{1}{h} + \frac{1}{q_e} t \quad (3)$$

Table 3. Comparison of the kinetic models for sorption of copper, zinc and nickel ions

Metal	Pseudo-first-order model				Pseudo-second-order model					Intra-particle diffusion		
	q _{e,exp.} (mg/g)	q _{e,calc.} (mg/g)	K _{ad}	R ²	q _{e,exp.} (mg/g)	q _{e,calc.} (mg/g)	k ₂	h	R ²	K _i	C _i	R ²
Cu ²⁺	25.00	1.758	0.143	0.98	25.00	24.95	0.164	102.25	0.99	1.04	22.19	0.99
Zn ²⁺	21.38	3.585	0.040	0.93	21.38	21.22	0.078	35.109	0.99	0.74	16.94	0.98
Ni ²⁺	20.10	4.47	0.043	0.94	20.10	20.04	0.038	15.196	0.99	0.99	14.41	0.96

In order to the higher porous structure and the good surface area (850m²/g) for granular activated carbon, there is a possibility of using intra-particle diffusion as the rate-limiting step for these sorption systems. The intra-particle diffusion model described by Weber and Morris (1963) [24] is expressed as:

$$q_t = K_i t^{0.5} + C_i \quad (4)$$

Where K_i and C_i are the intra-particle diffusion rate constant (mg/g min^{0.5}) and a constant, respectively. In Figure 10, the plot of q_t versus t^{0.5} gives a straight line at q_t before the equilibrium case with slope, K_i, and intercept, C_i, for all the studied cations. The values of K_i and C_i are listed in Table 3, where the intercept, C_i, is the portion of the extent of boundary layer thickness [2]. This indicates that the pore diffusion is not the only rate limiting step for sorption of cations onto OSAC-3. The higher K_i-values for all the cases indicate the enhancement of the sorption rate and best sorption mechanism, which is due to good bonding

Where k₂ (g mg⁻¹ min⁻¹) is the rate constant of the second-order model and h (k₂q_e²) is the initial adsorption rate constant. When the experimental data were applied into the second-order law, as shown in Figure 9, straight lines were obtained for all the studied cations. Different variables as the calculated and the experimental equilibrium uptake (q_{e,cal.} and q_{e,exp.}), the second-order rate constants (k₂), and the correlation coefficient (R²) were calculated and are shown in Table 3. As can be seen from Table 3, the calculated q_{e,cal.}-values are in agreement with the experimental q_{e,exp.}-data and they reflect higher correlation coefficients obtained in comparison with that obtained from the pseudo-first-order equation. This denotes that the sorption process follows the pseudo-second-order kinetic model and the chemisorption process may be the rate-limiting step, which involves valence forces through sharing or exchange of electrons between sorbent and sorbates [23]. In addition, Table 3 shows that the sorption rate constant, k₂, of Cu²⁺ ions is the highest value in comparison with the other investigated cations, which follow the order: Cu²⁺ > Zn²⁺ > Ni²⁺.

between the active groups on the sorbent surface and the studied cations [25].

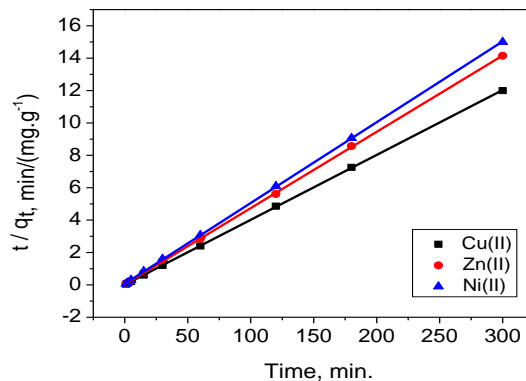


Fig. 9. Pseudo second order kinetic model for sorption of Cu²⁺, Zn²⁺ and Ni²⁺-ions on OSAC-3

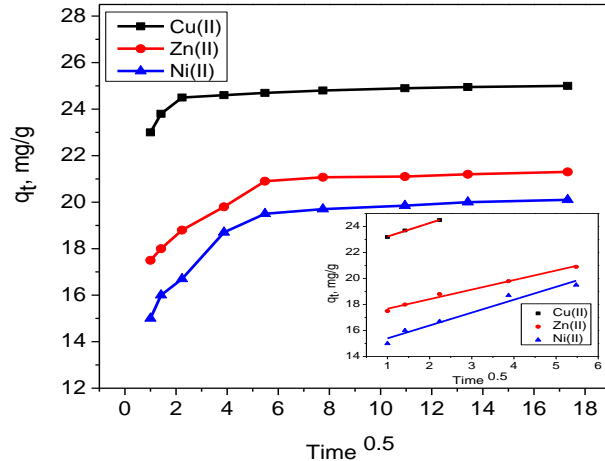


Fig. 10. Intra-particle diffusion plots for sorption of Cu^{2+} , Zn^{2+} and Ni^{2+} -ions on OSAC-3

After comparing the correlation coefficients (R^2) of the three kinetic models, the pseudo second order kinetic model is found to be the best model to fit the experiment data for all the investigated cations.

4.4. Equilibrium concentrations and sorption isotherms

The properties of sorption process depend not only on the properties of the sorbents, but also on the concentration of the metal ion solution. The initial metal ion concentration provides an important driving force to overcome all mass transfer resistances of the cations between aqueous solution and solid phase [26]. The effect of the initial concentration of heavy metal ions was studied at a pH of 5.7 and a shaking time of 2 hours. In Fig.5, it was noticed that the percentage removal efficiency values decreased from 97.7 % to 72.2% for Copper, 84% to 52% for Zinc, and 48.48% to 44% for Nickel, respectively, with an increase in the metal ion concentration from 5 to 25 mg/l by keeping all other parameters constant. Such a high efficiency of OSAC-3 toward the investigated ions make it applicable for the removal of $\text{Cu}(\text{II})$, $\text{Zn}(\text{II})$ and $\text{Ni}(\text{II})$ ions from low concentrated solutions such as those generated from painting/plating processes by Copper, Zinc, and Nickel metals. The effect of initial concentrations of heavy metal ions was studied and the isotherms are illustrated in Fig. 11. An adsorption isotherm is a basic representation showing the relationship between the amount adsorbed by a unit weight of adsorbent and the amount of adsorbate remaining in a test solution at equilibrium, Fig.11. It means it is the distribution of solute between the aqueous and solid phases at various equilibrium concentrations.

The obtained equilibrium sorption experimental data were tested using the commonly used Langmuir and Freundlich isotherm models. The Langmuir isotherm is based on the assumptions that: (i) all sites are equivalent; (ii) adsorption of solutes produces in monolayer coverage; (iii) the adsorbate molecule is adsorbed on a site independent of

the neighboring adsorbed molecules; (iv) coverage is independent of binding energy [27]. It is shown as follows:

$$\frac{1}{q_e} = \frac{1}{Q^o} + \frac{1}{(bQ^o)} \left(\frac{1}{C_e} \right) \quad (5)$$

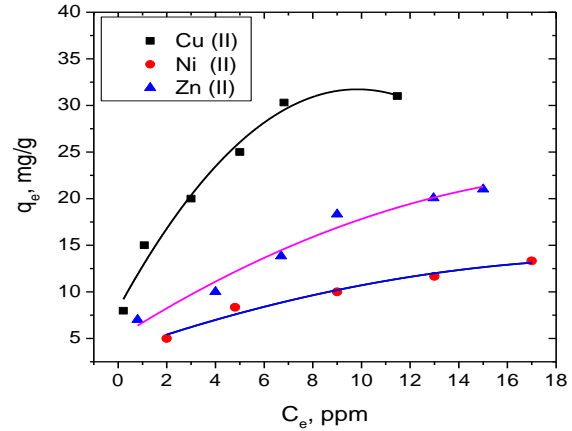


Fig. 11. Effect of initial solute concentration on sorption of Cu^{2+} , Zn^{2+} and Ni^{2+} on OSAC-3.

where q_e is the amount of metal ion sorbed per gram of the adsorbent at equilibrium in mg/g; C_e is the equilibrium concentration of metal ions left in solution at equilibrium in mg/l; Q^o is the maximum adsorption capacity in mg/g to form a complete monolayer coverage on the solid surface; and b is the Langmuir constant associated to the adsorption energy. Q^o and b have been calculated from the intercept, $1/Q^o$, and the slope, $1/(bQ^o)$, of plotting $1/q_e$ versus $1/C_e$, which give straight lines for all the investigated ions. The results are illustrated in Figure 12 (a). The essential characteristics and the feasibility of the Langmuir isotherm can be expressed by Hall et al. (1966) [22] in terms of a dimensionless constant separation factor R_L , which is defined as Eq. (6):

$$R_L = \frac{1}{1 + bC_o} \quad (6)$$

where C_o is the initial metal ion concentration (mg/l) and b is the Langmuir constant. The value of R_L is announced to the status of the adsorption isotherm to be either unfavorable ($R_L > 1$), linear ($R_L = 1$), favorable ($0 < R_L < 1$), or irreversible ($R_L = 0$). The R_L values are calculated for the adsorption of Cu^{2+} , Zn^{2+} and Ni^{2+} ions, and they are found to be 0.0243, 0.0571 and 0.5880, respectively. This indicates that the adsorption of Cu^{2+} , Zn^{2+} and Ni^{2+} on OSAC-3 are favorable. The Freundlich model is an empirical model which is based on the sorption on a heterogeneous surface with exponential variation active site energies. The linear form of the Freundlich isotherm model is expressed by the following equation [28]:

$$\log q_e = \log k_f + \frac{1}{n} \log C_e \quad (7)$$

Where k_f and n are empirical constants that indicate respectively adsorption capacity and adsorption intensity. Figure 12 (b) shows the linear plot of $\log q_e$ against $\log C_e$ for the adsorption of Cu^{2+} , Zn^{2+} and Ni^{2+} onto OSAC-3. The intercept and slope were used to calculate k_f and n -values, respectively. The Langmuir and Freundlich constants in addition with R^2 -values are given in Table (4). According to the regression coefficient values, R^2 , in Table 4, it can be determined that the adsorption isotherms can be well described by the Langmuir model rather than the Freundlich one for Cu^{2+} and Ni^{2+} ions. The opposite was shown for Zn^{2+} ions, where the experimental data were represented well by the Freundlich model rather than the Langmuir one. Furthermore, the experimental data for all the studied ions were represented by the Langmuir and Freundlich models because of the good R^2 -values for both of the investigated isotherm models. Therefore, the sorption of the cations was

attributed to the mixed mechanisms of ion-exchange as well as to the adsorption process.

According to Figure 13, an aqueous alkaline medium was obtained during the adsorption process, indicating that the ion exchange was the binding mechanism [29]. During the ion-exchange process, metal ions slipped through the pores and channels of the adsorbent material and replaced the elements in the OSAC-3 structure (potassium, calcium and magnesium, as shown in Table 2). In this work, the diffusion of ions was faster through the micro-pores of the OSAC-3 material; the ionic radii of the metal ions Cu^{2+} , Zn^{2+} and Ni^{2+} (0.72\AA , 0.74\AA and 0.69\AA , respectively) are smaller than the pores radii of the OSAC material (average OSAC-3 pore radius is 11\AA). According to the uptake amount and the maximum adsorption capacities, Q_o , the selectivity sequence of the studied metal ions by OSAC-3 can be given as $\text{Cu}^{2+} > \text{Zn}^{2+} > \text{Ni}^{2+}$. This is usually attributed to the differences in metal characteristics and the resultant affinity for sorption sites.

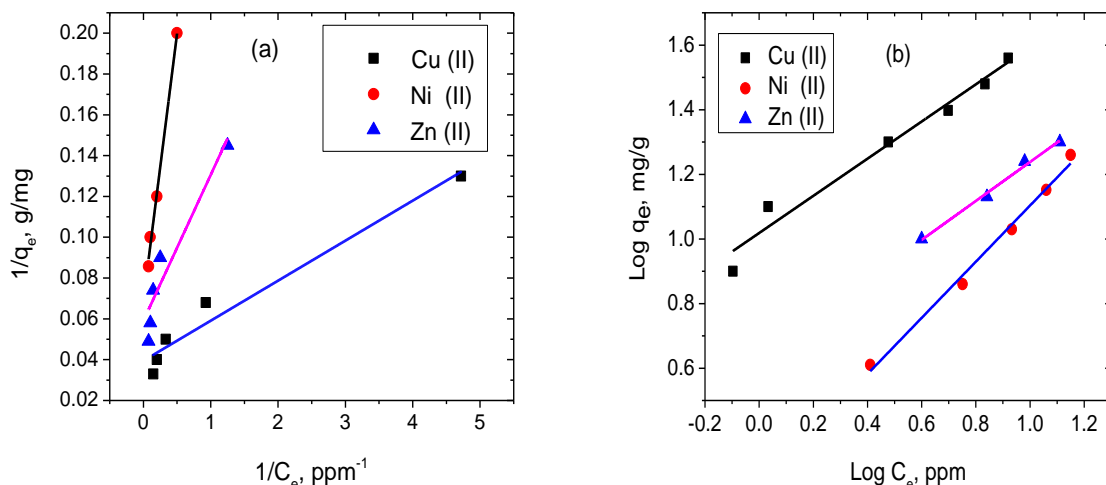


Fig. 12 (a,b). Langmuir and Freundlich plots of sorption of Cu^{2+} , Zn^{2+} and Ni^{2+} on OSAC-3.

Table 4. Langmuir and Freundlich constants with linear fit correlation coefficient (R^2).

Metal ions	Langmuir constants			Freundlich constants		
	Q_o	b	R^2	K_f	n	R^2
Cu^{2+}	25.381	2.010	0.980	12.830	1.740	0.951
Zn^{2+}	18.950	0.825	0.955	4.318	1.658	0.996
Ni^{2+}	14.650	0.259	0.993	3.809	2.252	0.983

Many investigators have tried to explain the action of the physicochemical properties of metal ions, as ionic radius, electron configuration and electronegativity on the mechanism of adsorption [30]. In this study, there was a linear relation between the metal ion uptake and the ionic radius of the ions. The ionic radius (r^i) of metal ions considered through this investigation takes the following order: K^+ ($r^i=1.38\text{\AA}$) $>$ Ca^{2+} ($r^i=1.02\text{\AA}$) $>$ Mg^{2+} ($r^i=0.86\text{\AA}$) $>$ Zn^{2+} ($r^i=0.74\text{\AA}$) $>$ Cu^{2+} ($r^i=0.72\text{\AA}$) $>$ Ni^{2+} ($r^i=0.69\text{\AA}$) $>$ H^+ ($r^i=0.154\text{\AA}$) [31]. Thus, all these heavy metal ions have a

smaller ionic radius than K^+ , Ca^{2+} and Mg^{2+} ions and the heavy metals can be incorporated in the molecular structure of OSAC-3 replacing K^+ , Ca^{2+} and Mg^{2+} ions from there, this is according to the cation exchange theory. A preferential sorption of Cu^{2+} ions against Zn^{2+} ions can be explained by the difference in the electronegativity (E), which was higher for Cu^{2+} ions ($E=1.90$) than for Zn^{2+} ions ($E=1.65$); also, the Pauling electronegativity for all the cations Cu^{2+} ($E=1.90$), Zn^{2+} ($E=1.65$) and Ni^{2+} ($E=1.91$) were higher than that for K^+ ($E=0.82$), Ca^{2+} ($E=1.0$) and Mg^{2+}

($E=1.31$). This indicated that all the investigated cations can replace K^+ , Ca^{2+} and Mg^{2+} ions [32], as shown in Fig.5. When taking the electronic configuration of Cu^{2+} ions into consideration, it was noticed that Cu^{2+} ions have one unpaired electron at the 3d-orbital as shown in Table (5); this means it is a paramagnetic metal. Subsequently, Cu^{2+} ions can be attracted by the magnetic field, possibly in the adsorbent in which the ash contained in the OSAC-3 has iron oxide. The main oxides content as tested by EDX is reported in Table 2. OSAC-3 had about 8 % ash content. On the other hand, the electronic configuration of Ni^{2+} and Zn^{2+} ions is stable, with no unpaired electrons at the 3d-orbital as shown in Table (5) and they will be repelled by a OSAC-3 magnetic field. This is perhaps one of the reasons for the lower adsorption capacity of OSAC-3 adsorbent for nickel and zinc ions in comparison to the adsorption of copper ions. The electronegativities (E) and ionic radii of Ni^{2+} , and Zn^{2+} are 1.91, 1.65 and 0.69, $0.74A^\circ$, respectively. The average electric dipole polarizabilities (D) of Ni, and Zn atoms are $6.8 \times 10^{-24} \text{ cm}^3$ and $7.1 \times 10^{-24} \text{ cm}^3$, respectively [33-34]. Puls and Bohn (1988) [34] explained the metal sorption

capacity using the concept of the conventional hard-soft acid-base (HSAB) principle.

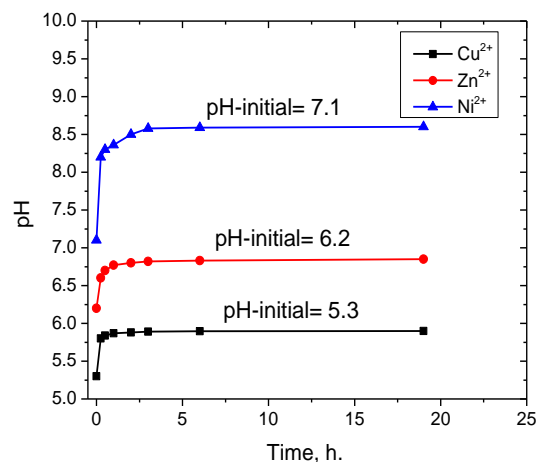


Fig. 13. Effect of time on changing of the initial pH of Cu^{2+} , Zn^{2+} and Ni^{2+} solution adsorbed on OSAC-3.

Table 5. Physicochemical properties of the cations

Character\ Ion	Cu^{2+}	Zn^{2+}	Ni^{2+}	K^+	Ca^{2+}	Mg^{2+}	H^+
Ionic radius, A°	0.720	0.740	0.690	1.380	1.020	0.860	0.154
Electron configuration	$3d^9 4s^2$	$3d^{10}$	$3d^8 4s^2$	$4s^1$	$4s^2$	$3s^2$	$1s^1$
Pauling electronegativity	1.90	1.65	1.91	0.82	1.00	1.31	---

According to the HSAB principle, hard Lewis acids choose to form complexes with hard Lewis bases, and soft acids prefer to make complexes with soft bases. The word “hard” means high electronegativity, low polarizability, and small ionic size, while vice-versa for “soft” ions. The sorption capacity of Ni^{2+} and Zn^{2+} by OSAC-3 follows the order of increasing ionic radii and polarizability as well as decreasing electronegativity and thus decreasing hardness. In this work, the OSAC-3 give a high adsorption of Zn^{2+} as softer ions compared with the less soft ions of Ni^{2+} . The OSAC-3 had a pH of 7.2, which means an alkaline surface of granular activated carbon OSAC-3. Therefore, OSAC-3 was used as a relatively soft Lewis base. The active sites of the adsorbent appeared to form the most stable complexes with the softer cations (as soft acid). Therefore, the adsorbent surface has a high ability for complexation towards the soft acids (as Zn^{2+} ions) [35]. Hence, the sequence of metal sorption capacities in this research was found as $Cu^{2+} > Zn^{2+} > Ni^{2+}$. A comparison of the maximum sorption capacity of $Cu(II)$, $Zn(II)$ and $Ni(II)$ and the surface area of the investigated OSAC-3 with other activated carbons derived from other precursors with different activation methods is shown in Table 6. Generally, OSAC-3 has a good surface area with a higher sorption capacity for $Cu(II)$, $Zn(II)$ and $Ni(II)$ than other precursors; thus, it was recommended to use OSAC-3 for the removal of $C(II)$, $Zn(II)$ and $Ni(II)$ -ions from aqueous solutions.

4.5. Thermodynamics study

Temperature is one of the important parameters affecting the rate of the sorption process. To study the effect of the temperature (285, 298, 308 and 323 K) on the adsorption of $Cu(II)$, $Zn(II)$ and $Ni(II)$ ions, the experiments were carried out at constant concentrations of 20 mg/L for all the investigated cations. The data showed that by increasing the temperature from 285K to 323K, the uptake decreased from 29.43mg/g to 24.55mg/g for $Cu(II)$ ions. And the adsorption of $Zn(II)$ and $Ni(II)$ increased from 18.52mg/g to 20.70mg/g and from 16.05mg/g to 20.18mg/g, respectively. To study the nature of the adsorption process, the thermodynamic parameters of free energy change (ΔG°), enthalpy change (ΔH°), and entropy change (ΔS°) were calculated using the following equations:

$$\Delta G^\circ = -RT \ln K_c \quad (8)$$

$$\log K_c = \left(\frac{\Delta S^\circ}{2.303} \right) - \left(\frac{\Delta H^\circ}{2.303R} \right) \left(\frac{1}{T} \right) \quad (9)$$

$$\Delta G^\circ = \Delta H^\circ - T \Delta S^\circ \quad (10)$$

where R is the gas constant ($8.3143 \text{ JK}^{-1} \text{ mol}^{-1}$), T is the absolute temperature in Kelvin and K_c is the equilibrium constant. K_c -values are calculated as the distribution of the cations between solid surface and solution ($K_c = \frac{q_e}{C_e}$).

The values of ΔG° were calculated from Eq. (8) at different temperatures and the ΔH° -values were obtained from the slope of a plot $\log K_c$ versus $1/T$ (Fig. 14) according to Eq. (9) as linear regression analysis. The ΔS° -values were calculated from Eq. (10). The values of the studied thermodynamic parameters are given in Table 7. The enthalpy of the adsorption, ΔH° , is a measure of the energy barrier that must be overcome by the reacting cations [50].

The positive value of ΔH° for Zn^{2+} and Ni^{2+} ions suggests that the adsorption reactions onto the adsorbent are endothermic in nature, but for Cu^{2+} ions, the negative value of ΔH° means an exothermic reaction on the adsorbent surface. Therefore, this means that increasing temperature will favor the adsorption of Zn^{2+} and Ni^{2+} ions and hinder the adsorption for Cu^{2+} ions onto the adsorbent.

Table 6. Surface areas and maximum metal ions (Ni(II), Cu(II) and Cd(II)) adsorption capacity of the activated carbons derived from different carbon precursors by different activation methods.

Carbon precursor	Activating agent	Surface area (m ² /g)	Q _{max} (mg/g)			Reference
			Cu(II)	Zn(II)	Ni(II)	
Phragmites australis	H ₃ PO ₄	894.5	5.421		22.88	[34]
	(NH ₃) ₃ PO ₄	444.9	6.982		34.04	[34]
	(NH ₃) ₂ HPO ₄	495.7	6.429		31.81	[34]
	NH ₃ H ₂ PO ₄	408.5	6.213		31.40	[34]
Commercial GAC (F 400)	---	960			3.12	[35]
Commercial GAC (F 200)	---	790	24.10			[36]
<i>Ceiba pentandra</i>	Steam	521	20.8			[37]
Commercial carbon	Tannic acid	325.1	2.23			[38]
Apricot	K ₂ CO ₃	770			32.36	[39]
Briquette	Steam	719			18.79	[40]
Almond husk	H ₂ SO ₄				37.17	[41]
Hazelnut shell	H ₂ SO ₄	441			11.64	[42]
Local wood	--	1400		20.52		[43]
coconut shell (ACABPEX.)	Potassium ethyl xanthate with 4 M nitric acid solution	804.0		17.544		[44]
Residual from solvent extracted olive pulp (ACOP)	steam/nitrogen mixture	364		32.68		[45]
Olive stone (ACO)	steam/N ₂ mixture	474		16.08		[45]
Apricot stone (ACA)	steam/N ₂ mixture	486		13.175		[45]
Peach stone (ACP)	steam/N ₂ mixture	660		6.370		[45]
apple pulp	ZnCl ₂ / N ₂ gas	1067.1		11.72		[46]
olive oil industrial solid waste	N ₂ /steam gas	850	25.381	18.950	14.650	The present work

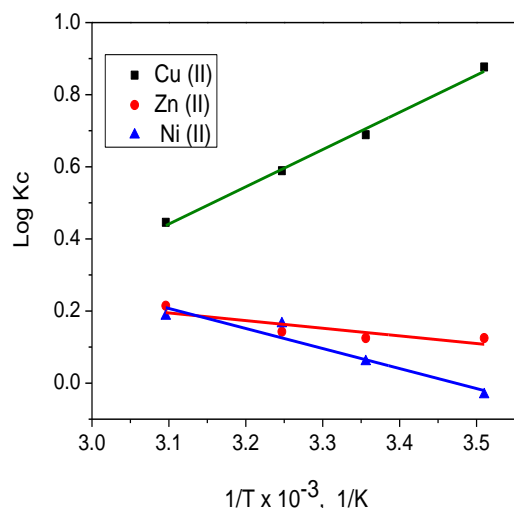


Fig. 14. Effect of temperature on the distribution coefficient

The positive entropy change (ΔS°) values for all the studied cation at all investigated temperatures, except for Ni^{2+} ions at 285K, showed an increase in the randomness at the solid/solution interface during the sorption process. On the other hand, the negative entropy change value for Ni^{2+} ions at 285K corresponded to a decrease in the degree of freedom of the adsorbed nickel species. The degree of freedom decreased with a decrease in temperature for Zn^{2+} and Ni^{2+} ions, the opposite was noticed for the sorption of Cu^{2+} -ions.

Negative ΔG° -values indicated a spontaneous nature of sorption process for all the studied cations at all the investigated temperatures except at a temperature of 285K for Ni^{2+} -ions. The negativity of ΔG° -values decreased with decreasing temperature for Zn^{2+} and Ni^{2+} ions, the opposite was noticed for Cu^{2+} ions. On the other hand, positive or small negative values of Free energy change (ΔG°) could

suggest that the reaction required a small amount of energy. It can be seen from Table 7 that the ΔG° are positive for Ni^{2+} at 285K, while a low negative-value under other temperatures for Ni^{2+} and Zn^{2+} meant that small external energy input was needed for the adsorption process of Ni^{2+} and Zn^{2+} ions on OSAC-3. This was confirmed by the less

positive values of ΔH° . On the other hand, high negative values of ΔG° for Cu^{2+} ions suggested a spontaneous adsorption reaction with no need for external energy, and this was supported by the high negative values of ΔH° .

Table 7. Thermodynamic parameters for the cations adsorption on OSAC-3.

T, K.	Cu^{2+}			Zn^{2+}			Ni^{2+}		
	ΔG°	ΔH°	ΔS°	ΔG°	ΔH°	ΔS°	ΔG°	ΔH°	ΔS°
285	-4.78		16.72	-0.53		1.86	0.18		-0.58
298	-3.93		13.12	-0.71		2.39	-0.34		1.19
308	-3.48	-19.77	11.23	-0.84	4.06	2.75	-0.97	10.63	3.19
232	-2.76		8.48	-1.33		4.12	-1.15		3.6

5. Conclusions

In the present study, the removal of Cu^{2+} , Zn^{2+} and Ni^{2+} ions from aqueous solution by adsorption on olive stone activated carbon via batch technique was investigated. Microporous OSAC-3 material with a high surface area of $850\text{m}^2/\text{g}$ was obtained from physical activated olive stone waste. The results showed that the removal of the three cations was favorable at a higher pH, but the kinetic, isotherms, and thermodynamic studies were operated at a pH of 5.7 to ensure that no precipitation occurred for the studied cations. It was observed that during adsorption of the three cations, an increase in the solution pH was noticed with agitation time. This indicated that there was an ion-exchange mechanism occurring simultaneous with the adsorption of Cu^{2+} , Zn^{2+} and Ni^{2+} ions on the active sites of OSAC-3 surface. The rate of adsorption for the three elements was very fast in the first 5min., reaching equilibrium after 30min. for Cu^{2+} -ions, after 60min. for Zn^{2+} , and after 120min. for Ni^{2+} ions adsorption. The experimental data were successfully described by the pseudo-second order model. The intra-particle diffusion model showed that the adsorption mechanism of Cu^{2+} , Zn^{2+} and Ni^{2+} ions was a complex mechanism, where the intra-particle diffusion participated in the overall rate of the adsorption process, and it was not the only rate-determining step. The equilibrium adsorption data was described by both Langmuir and Freundlich models and the adsorption capacity of OSAC-3 decreased in the following sequence: $25.381\text{ mgCu}^{2+}/\text{g} > 18.950\text{ mgZn}^{2+}/\text{g} > 14.650\text{ mgNi}^{2+}/\text{g}$. The thermodynamic parameters showed that the negative values of ΔG for the three metals (except for adsorption of Ni^{2+} ions at temperature 285K) indicated spontaneous adsorption of the cations onto OSAC-material. The positive ΔH -values of Zn^{2+} and Ni^{2+} ions confirmed the endothermic adsorption process while the negative value of ΔH referred to the exothermic nature for the sorption process for Cu^{2+} ions. Therefore, the temperature increased

the adsorption of Zn^{2+} and Ni^{2+} ions at equilibrium and hindered the adsorption of Cu^{2+} ions onto OSAC-3. The positive values of ΔS for all the studied cations (except for adsorption of Ni^{2+} ions at 285K) clarified an increase in the randomness at solid/solution interface during the adsorption process. The obtained results indicated that OSAC-3 has the potential to be used as a low-cost material for the sorption of Cu^{2+} , Zn^{2+} and Ni^{2+} ions from aqueous media.

Acknowledgment

The author would like to thank the chairman of the olive oil factory in the Wahet Sewa region in Egypt for supplying the olive oil industrial solid waste.

References

- [1] Jayakumar, R., Rajasimman, M., Karthikeyan, C. (2015). Optimization, equilibrium, kinetic, thermodynamic and desorption studies on the sorption of Cu (II) from an aqueous solution using marine green algae: *Halimeda gracilis*. *Ecotoxicology and environmental safety*, 121, 199-210.
- [2] Kula, I., Uğurlu, M., Karaoğlu, H., Celik, A. (2008). Adsorption of Cd (II) ions from aqueous solutions using activated carbon prepared from olive stone by ZnCl₂ activation. *Bioresource technology*, 99(3), 492-501.
- [3] Meena, A. K., Mishra, G. K., Rai, P. K., Rajagopal, C., Nagar, P. N. (2005). Removal of heavy metal ions from aqueous solutions using carbon aerogel as an adsorbent. *Journal of hazardous materials*, 122(1), 161-170.
- [4] Depci, T., Kul, A. R., Önal, Y. (2012). Competitive adsorption of lead and zinc from aqueous solution on activated carbon prepared from Van apple pulp: study in single-and multi-solute systems. *Chemical engineering journal*, 200, 224-236.
- [5] Koplan, J. P. (1999). Toxicological profile for Chlorophenols. Agency for Toxic Substances and

- Disease Registry (ATSDR), US Department of Health and Human Services. *Public Health Service*.
- [6] Bohli, T., Ouederni, A., Fiol, N., Villaescusa, I. (2015). Evaluation of an activated carbon from olive stones used as an adsorbent for heavy metal removal from aqueous phases. *Comptes rendus chimie*, 18(1), 88-99.
- [7] Hafshejani, L. D., Nasab, S. B., Gholami, R. M., Moradzadeh, M., Izadpanah, Z., Hafshejani, S. B., Bhatnagar, A. (2015). Removal of zinc and lead from aqueous solution by nanostructured cedar leaf ash as biosorbent. *Journal of molecular liquids*, 211, 448-456.
- [8] Rivera-Utrilla, J., Sánchez-Polo, M., Gómez-Serrano, V., Alvarez, P. M., Alvim-Ferraz, M. C. M., Dias, J. M. (2011). Activated carbon modifications to enhance its water treatment applications. An overview. *Journal of hazardous materials*, 187(1), 1-23.
- [9] Alslaibi, T. M., Abustan, I., Ahmad, M. A., Abu Foul, A. (2013). Effect of different olive stone particle size on the yield and surface area of activated carbon production. In *Advanced materials research* (Vol. 626, pp. 126-130). Trans tech publications.
- [10] Awwad, N. S., El-Zahhar, A. A., Fouda, A. M., Ibrahim, H. A. (2013). Removal of heavy metal ions from ground and surface water samples using carbons derived from date pits. *Journal of environmental chemical engineering*, 1(3), 416-423.
- [11] Alslaibi, T. M., Abustan, I., Ahmad, M. A., Foul, A. A. (2013). Review: Comparison of agricultural by-products activated carbon production methods using surface area response. *CJASR*, 2, 18-27.
- [12] Alslaibi, T. M., Abustan, I., Ahmad, M. A., Foul, A. A. (2013). A review: production of activated carbon from agricultural byproducts via conventional and microwave heating. *Journal of chemical technology and biotechnology*, 88(7), 1183-1190.
- [13] Alslaibi, T. M., Abustan, I., Ahmad, M. A., Foul, A. A. (2014). Kinetics and equilibrium adsorption of iron (II), lead (II), and copper (II) onto activated carbon prepared from olive stone waste. *Desalination and water treatment*, 52(40-42), 7887-7897.
- [14] Lin, L., Zhai, S. R., Xiao, Z. Y., Song, Y., An, Q. D., Song, X. W. (2013). Dye adsorption of mesoporous activated carbons produced from NaOH-pretreated rice husks. *Bioresource technology*, 136, 437-443.
- [15] Olèico (2009) European awareness raising campaign for an environmentally sustainable olive mill waste management. available at LIFE07 INF/IT/000438
- [16] Ghanbari, R., Anwar, F., Alkharfy, K. M., Gilani, A. H., Saari, N. (2012). Valuable nutrients and functional bioactives in different parts of olive (*Olea europaea* L.) — a review. *International journal of molecular sciences*, 13(3), 3291-3340.
- [17] Daifullah, A. H. M., Rizk, M. A., Aly, H. M., Yakout, S. M., Hassen, M. R. Treatment of some organic pollutants (THMs) using activated carbon derived from local agro-residues.
- [18] Puziy, A. M., Poddubnaya, O. I., Martínez-Alonso, A., Castro-Muniz, A., Suárez-García, F., Tascón, J. M. (2007). Oxygen and phosphorus enriched carbons from lignocellulosic material. *Carbon*, 45(10), 1941-1950.
- [19] Jayakumar, R., Rajasimman, M., Karthikeyan, C. (2015). Optimization, equilibrium, kinetic, thermodynamic and desorption studies on the sorption of Cu (II) from an aqueous solution using marine green algae: *Halimeda gracilis*. *Ecotoxicology and environmental safety*, 121, 199-210.
- [20] Beveridge, T. J. (1986). Biotechnology and bioengineering symposium No. 16: Biotechnology for the mining, metal-refining, and fossil fuel processing industries.
- [21] Ho, Y. S., & McKay, G. (1999). The sorption of lead (II) ions on peat. *Water research*, 33(2), 578-584.
- [22] Hall, K. R., Eagleton, L. C., Acrivos, A., Vermeulen, T. (1966). Pore-and solid-diffusion kinetics in fixed-bed adsorption under constant-pattern conditions. *Industrial & engineering chemistry fundamentals*, 5(2), 212-223.
- [23] Aksas, H., Bouregghda, M.Z., Babaci, H. and Louhab, K. (2015) Kinetics and Thermodynamics of Cr Ions Sorption on Mixed Sorbents prepared from Olive Stone and Date pit from Aqueous Solution. *International journal of food and biosystem engineering*, 1(1), 1-8.
- [24] Weber, W. J., Morris, J. C. (1963). Kinetics of adsorption on carbon from solution. *Journal of the sanitary engineering division*, 89(2), 31-60.
- [25] John, A. C., Ibrionke, L. O., Adedeji, V., Oladunni, O. (2011). Equilibrium and kinetic studies of the biosorption of heavy metal (cadmium) on *Cassia siamea* Bark. *American-Eurasian journal of scientific research*, 6(3), 123-130.
- [26] Aksu, Z., Akpınar, D. (2000). Modelling of simultaneous biosorption of phenol and nickel (II) onto dried aerobic activated sludge. *Separation and purification technology*, 21(1), 87-99.
- [27] Langmuir, I. (1916). The constitution and fundamental properties of solids and liquids. *J. Am. Journal of the American chemical society*, 38(11), 2221-2295.
- [28] Uber, F. H. (1985). Die adsorption in losungen. *Zeitschrift for physikalische chemie*, 57, 387-470.
- [29] Brady, J. M., Tobin, J. M. (1994). Adsorption of metal ions by *Rhizopus arrhizus* biomass: Characterization studies. *Enzyme and microbial technology*, 16(8), 671-675.
- [30] Şengil, İ. A., Özacar, M. (2009). Competitive biosorption of Pb²⁺, Cu²⁺ and Zn²⁺ ions from aqueous solutions onto valonia tannin resin. *Journal of hazardous materials*, 166(2), 1488-1494.
- [31] Shannon, R. T. (1976). Revised effective ionic radii and systematic studies of interatomic distances in halides

- and chalcogenides. *Acta crystallographica section A: Crystal physics, diffraction, theoretical and general crystallography*, 32(5), 751-767.
- [32] Gorgievski, M., Božić, D., Stanković, V., Štrbac, N., Šerbula, S. (2013). Kinetics, equilibrium and mechanism of Cu^{2+} , Ni^{2+} and Zn^{2+} ions biosorption using wheat straw. *Ecological engineering*, 58, 113-122.
- [33] Liu, C. L., Chang, T. W., Wang, M. K., Huang, C. H. (2006). Transport of cadmium, nickel, and zinc in Taoyuan red soil using one-dimensional convective–dispersive model. *Geoderma*, 131(1), 181-189.
- [34] Puls, R. W., Bohn, H. L. (1988). Sorption of cadmium, nickel, and zinc by kaolinite and montmorillonite suspensions. *Soil science society of America journal*, 52(5), 1289-1292.
- [35] Sullivan, P. J. (1977). The principle of hard and soft acids and bases as applied to exchangeable cation selectivity in soils. *Soil science*, 124(2), 117-121.
- [36] Guo, Z., Fan, J., Zhang, J., Kang, Y., Liu, H., Jiang, L., Zhang, C. (2016). Sorption heavy metal ions by activated carbons with well-developed microporosity and amino groups derived from *Phragmites australis* by ammonium phosphates activation. *Journal of the Taiwan institute of chemical engineers*, 58, 290-296.
- [37] Nguyen, T. A. H., Ngo, H. H., Guo, W. S., Zhang, J., Liang, S., Yue, Q. Y., Nguyen, T. V. (2013). Applicability of agricultural waste and by-products for adsorptive removal of heavy metals from wastewater. *Bioresource technology*, 148, 574-585.
- [38] Ozsoy, H. D., Kumbur, H., Saha, B., Van Leeuwen, J. H. (2008). Use of *Rhizopus oligosporus* produced from food processing wastewater as a biosorbent for Cu (II) ions removal from the aqueous solutions. *Bioresource technology*, 99(11), 4943-4948.
- [39] Rao, M. M., Ramesh, A., Rao, G. P. C., Seshaiyah, K. (2006). Removal of copper and cadmium from the aqueous solutions by activated carbon derived from *Ceiba pentandra* hulls. *Journal of hazardous materials*, 129(1), 123-129.
- [40] Üçer, A., Uyanik, A., Aygün, Ş. F. (2006). Adsorption of Cu (II), Cd (II), Zn (II), Mn (II) and Fe (III) ions by tannic acid immobilised activated carbon. *Separation and purification technology*, 47(3), 113-118.
- [41] Erdoğan, S., Önal, Y., Akmil-Başar, C., Bilmez-Erdemoğlu, S., Sarıcı-Özdemir, Ç., Köseoğlu, E., Içduygu, G. (2005). Optimization of nickel adsorption from aqueous solution by using activated carbon prepared from waste apricot by chemical activation. *Applied surface science*, 252(5), 1324-1331.
- [42] Wilson, K., Yang, H., Seo, C. W., Marshall, W. E. (2006). Select metal adsorption by activated carbon made from peanut shells. *Bioresource technology*, 97(18), 2266-2270.
- [43] Hasar, H. (2003). Adsorption of nickel (II) from aqueous solution onto activated carbon prepared from almond husk. *Journal of hazardous materials*, 97(1), 49-57.
- [44] Demirbaş, E., Kobya, M., Öncel, S., Şencan, S. (2002). Removal of Ni (II) from aqueous solution by adsorption onto hazelnut shell activated carbon: equilibrium studies. *Bioresource technology*, 84(3), 291-293.
- [45] Kouakou, U., Ello, A. E. S., Yapo, J. A., Trokourey, A. (2013). Adsorption of iron and zinc on commercial activated carbon. *Journal of environmental chemistry and ecotoxicology*, 5(6), 168-171.
- [46] Behnamfard, A., Salarirad, M. M., Vegliò, F. (2014). Removal of Zn (II) ions from aqueous solutions by ethyl xanthate impregnated activated carbons. *Hydrometallurgy*, 144, 39-53.
- [47] Galiatsatou, P., Metaxas, M., Kasselouri-Rigopoulou, V. (2002). Adsorption of zinc by activated carbons prepared from solvent extracted olive pulp. *Journal of hazardous materials*, 91(1), 187-203.
- [48] Depci, T., Kul, A. R., Önal, Y. (2012). Competitive adsorption of lead and zinc from aqueous solution on activated carbon prepared from Van apple pulp: study in single-and multi-solute systems. *Chemical engineering journal*, 200, 224-236.
- [49] Alslaihi, T. M., Abustan, I., Ahmad, M. A., Abu Foul, A. (2014). Preparation of activated carbon from olive stone waste: optimization study on the removal of Cu^{2+} , Cd^{2+} , Ni^{2+} , Pb^{2+} , Fe^{2+} , and Zn^{2+} from aqueous solution using response surface methodology. *Journal of dispersion science and technology*, 35(7), 913-925.
- [50] Unuabonah, E. I., Adebowale, K. O., Olu-Owolabi, B. I., Yang, L. Z., Kong, L. (2008). Adsorption of Pb (II) and Cd (II) from aqueous solutions onto sodium tetraborate-modified Kaolinite clay: equilibrium and thermodynamic studies. *Hydrometallurgy*, 93(1), 1-9.